

Probing Field Emission from Boron Carbide Nanowires *

TIAN Ji-Fa(田继发)¹, BAO Li-Hong(鲍丽宏)¹, WANG Xing-Jun(王兴军)¹, HUI Chao(惠超)¹,
LIU Fei(刘飞)², LI Chen(李晨)¹, SHEN Cheng-Min(申承民)¹, WANG Zong-Li(王宗立)¹,
GU Chang-Zhi(顾长志)¹, GAO Hong-Jun(高鸿钧)^{1**}

¹Beijing National Laboratory for Condensed Matter Physics, Institute of Physics, Chinese Academy of Sciences,
Beijing 100190

²Laboratory for State Key Laboratory of Optoelectronic Materials and Technologies, School of Physics and
Engineering, Sun Yat-sen University, Guangzhou 510275

(Received 10 March 2008)

High density boron carbide nanowires are grown by an improved carbon thermal reduction technique. Transmission electron microscopy and electron energy loss spectroscopy of the sample show that the synthesized nanowires are B₄C with good crystallization. The field emission measurement for an individual boron nanowire is performed by using a Pt tip installed in the focused ion beam system. A field emission current with enhancement factor of 10⁶ is observed and the evolution process during emission is also carefully studied. Furthermore, a two-step field emission with stable emission current density is found from the high-density nanowire film. Our results together suggest that boron carbide nanowires are promising candidates for electron emission nanodevices.

PACS: 81.07.-b, 73.63.-b

Boron carbide (B₄C) is one of the important lightweight and high temperature refractory materials.^[1,2] It can be used for neutron absorbent, high-temperature thermoelectric energy conversion, and field emission display.^[3] Recently, nanostructured boron carbide has attracted much attention due to its potential reinforcing phase in ceramic or metal matrix composites and in sliding wear,^[4] and its higher and stronger mechanical properties.^[5] One-dimensional nanostructures of B₄C have been synthesized by reaction of carbon nanotubes with boron oxide vapour,^[6-8] pyrolyzing method,^[9] plasma-enhanced chemical vapour deposition,^[10] and carbon thermal reduction method.^[11] Despite these progresses, the structure and property could not be well controlled, which limits the properties investigation and the practical applications. Therefore, there still needs more efforts to find a convenient way to prepare 1D boron carbide nanostructures.

In this Letter, we report the synthesis of high density boron carbide nanowires on Si(111) surface via an improved carbon thermal reduction by introducing boron powder with Fe₃O₄ nanoparticles as catalyst at 1100°C. We investigate the field emission properties from a single nanostructured boron carbide for the first time and the evolution processes during emission are also observed. Furthermore, the high density boron carbide nanowire film show interesting field emission properties.

The catalyst, 6–8 nm Fe₃O₄ nanoparticles, was synthesized by high temperature solution phase reaction.^[12] The preparation of substrate is as follows: First, some boron powder was mixed with the Fe₃O₄ catalyst solution and dispersed by ultrasonication for 30 s; then, the mixed solution was dropped

onto a silicon (111) substrate. Boron powder, boron oxide (B₂O₃) and carbon black were the source materials and were mixed adequately with a mass ratio of 2:1:1. The precursors were put into a ceramic boat and the substrate was put on the ceramic boat with its surface facing directly to the precursors. The reaction boat was placed in the furnace centre and high purity argon gas was purged at a flow rate of 300 sccm for 0.5 h to remove air. The furnace temperature was raised from room temperature to 250°C at a rate of 17°C/min and kept for 30 min to remove organic ligands and moisture from the catalyst. After that, the flow rate of carrier gas was changed to 30 sccm and the temperature was increased to 1100°C at a rate of 10°C/min and kept it for 4 h before the furnace was cooled down to room temperature naturally. High density boron carbide nanowires were obtained on the silicon wafer.

A field-emission type scanning electron microscope (SEM; Model XL-SFEG, FEI Corp., Hillsboro, OR) and a transmission electron microscopy (TEM; Model 200CX; JEOL, Tokyo, Japan) and high resolution transmission electron microscopy (HRTEM; Tecnai F20; FEI Co.) were used to investigate morphology and microstructures, respectively. Electron energy loss spectroscopy (EELS) was used to identify the chemical compositions of the nanostructures. The elemental distribution was performed by energy filter transmission electron microscopy (EFTEM). The field emission measurement on a single nanowire was performed in focused ion beam (FIB; DB235; FEI Co.) system with a Pt probe. Field emission experiments on high density nanowire film were carried out in a vacuum chamber at room temperature. A molybdenum tip was adopted as an anode. Emission current

*Supported partially by the National High-Tech Research and Development Programme of China under Grant No 2007AA03Z305 and the National Key Basic Research Programme of China under Grant No 2007CB935503 and CAS/SAFEA International Cooperation.

**Email: hjgao@aphy.iphy.ac.cn

© 2008 Chinese Physical Society and IOP Publishing Ltd

was measured by a picoammeter (Keithley 485).

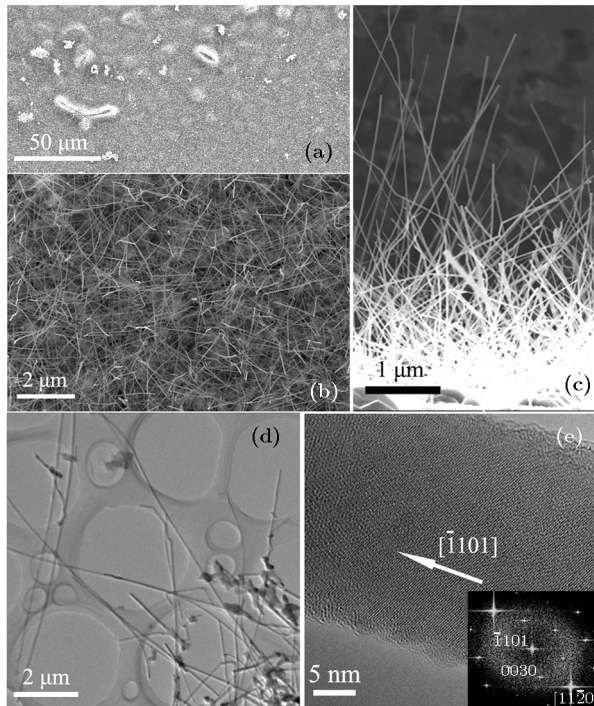


Fig. 1. Morphology and structure of boron carbide nanowires. (a) The SEM image of large-scale boron carbide nanowires. (b) The SEM image of high density boron carbide nanowires with higher magnification. (c) The side-view SEM image showing some protrusions of boron carbide nanowires. (d) The TEM image of boron carbide nanowires. (e) The HRTEM image of boron carbide nanowire, the inset is the corresponding FFT pattern from the HRTEM image.

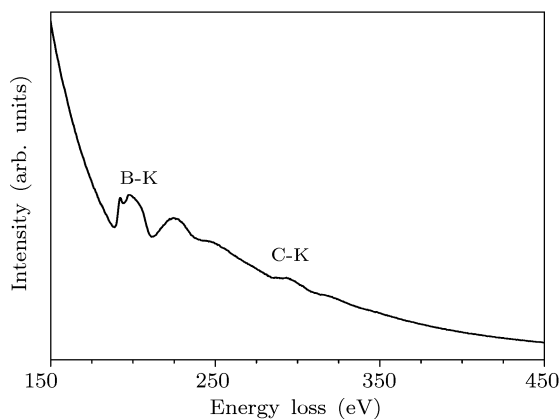


Fig. 2. EELS core electron K-shell spectra from boron carbide nanowire showing characteristic B and C K-edges at 188 eV and 284 eV.

Figure 1(a) displays SEM image of large-scale high density nanowires on a Si (111) substrate and Fig. 1(b) is the high resolution SEM image of the boron carbide nanowires. The cross-section view of the nanowires shows that high density nanowires at the bottom almost have the same height, but there are some low density protrusions (Fig. 1(c)). The nanowires have diameters in range 20–30 nm and lengths in microme-

tres. The TEM image (Fig. 1(d)) of the nanowires indicates that the nanowires grow from the boron powder and Fe-cluster catalyst. The HRTEM image (Fig. 1(e)) of a single boron carbide nanowire gives the crystal lattice fringes. The inset image in Fig. 1(e) is the two-dimensional fast Fourier transformation (FFT) of the lattice-resolved image obtained from the corresponding HRTEM image. It reveals that the crystalline B_4C nanowires grow in the $[\bar{1}101]$ direction.

The chemical compositions of boron carbide nanowires were analysed by electron energy loss spectroscopy (EELS). Figure 2 shows the typical EELS spectrum from the nanowires. The characteristic B and C K-edges at 188 eV and 284 eV are clearly visible. The observed K-edges correspond to sp^2 bonded B and C atoms, with B/C ratio of 4.08, which is consistent with a stoichiometry of B_4C .

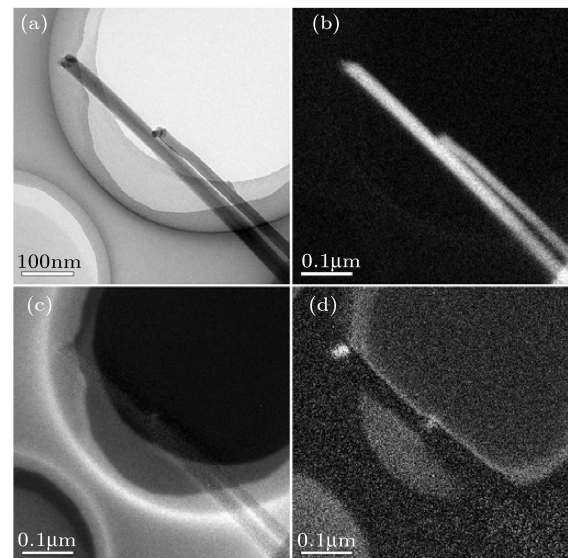


Fig. 3. Energy filter mapping results of the boron carbide nanowires. (a) The TEM image of the product. (b) The mapping image of boron. (c) The mapping image of carbon. (d) The mapping image of iron.

To investigate the elemental distribution in B_4C nanowires, an energy filter test was carried out. The typical TEM image of the nanowires is shown in Fig. 3(a). The energy filter mapping image of boron (Fig. 3(b)) shows that it uniformly located along the longitudinal direction of the two nanowires. Figure 3(c) shows a weak profile of the energy filter mapping of carbon located at the same position as boron. Because the concentration of carbon in the nanowires is much lower than that of the carbon film of the Cu grid, the mapping profile of carbon is not conclusive. Figure 3(d) is the energy filter mapping image of iron, which shows that it only exists at the tip of this nanostructure. This further indicates that the growth mechanism of the boron carbide nanowires may follow the vapour–liquid–solid (VLS)^[13] process.

In order to investigate the nature of field emission from individual boron carbide nanowires, the boron

carbide nanowire film was mounted on the sample holder of the FIB system. The Pt probe equipped in the system not only provides an exact localizer, but also gives one electrode. With this configuration a field emitted current was detected from 42 V, and increases monotonically without showing any saturation as shown in Fig. 4(b). The emission current is achieved $1.5 \mu\text{A}$ at an applied voltage of 80 V. This result is better than that of other reported Bi_2O_3 , In-doped ZnO, LaB_6 and TaSi_2 nanowires^[14–17] so far and compatible to those of the multi-wall carbon nanotubes.^[18,19] The Fowler–Nordheim (F-N) plot, $\ln(I/V^2)$ vs $1/V$, is shown in the inset of Fig. 4(b). The linearity of the plot suggests that the field emission from boron carbide nanowire emitter agrees with a metal-vacuum field emission (F-N) model. The slope k of the F-N plot, where $k = -6.44 \times 10^7 \phi_3/2/\beta$, can be used to estimate the enhancement factor of boron carbide nanowire. If we assume that the work function ϕ_B is between 4 and 5 eV, the enhancement factor β is about 10^6 .

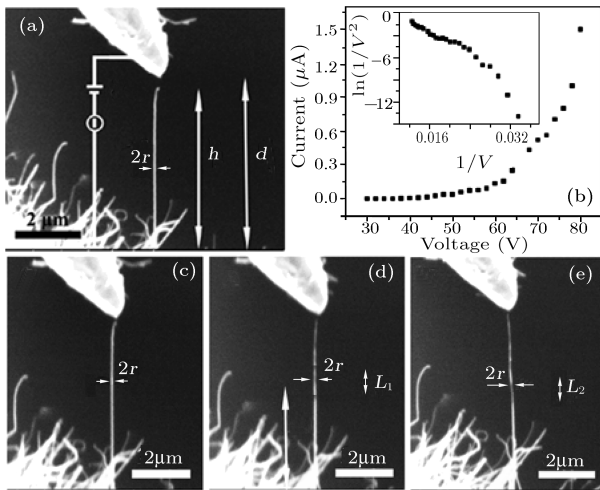


Fig. 4. (a) SEM image of a boron carbide nanowire of length $h = 5 \mu\text{m}$ and radius $r = 15 \text{ nm}$ with the Pt sharp anode positioned at a distance $d = 5.35 \mu\text{m}$. (b) Corresponding $I - V$ curve, inset is the FN plot. (c)–(e) The evolution process of a boron carbide nanowire during FE, $h_1 = 2.7 \mu\text{m}$, $L_1 = 590 \text{ nm}$, $L_2 = 1.3 \mu\text{m}$.

For further analysis of the field emission process, we gradually increased the bias voltage for the same nanowire in Fig. 4(c). When the bias voltage is 90 V, the diameters at the top and the position (indicated by arrows) of h_1 of the nanowire (Fig. 4(d)) becomes thinner than that of the original wire. From Figs. 4(d) and 4(e), the length (l_1 and l_2) of the region with thinner diameter was enlarged with the increasing voltage. Then, the upper part of the boron carbide nanowire was burned away gradually. Finally, it was removed completely at the position shown by arrows. From these investigations, it can be concluded that the failure of the boron carbide emitter tends to take place at an interior point rather than at the tip of the boron carbide nanowire.

We further measured the field emission property

of the high density B_4C nanowire film as shown in Fig. 5. It exhibits a two-step field emission property from the plot of FE current density J as a function of the applied electric field E . The FE current density J is turned on at $4.0 \text{ V}/\mu\text{m}$ and steadily increases to $2.48 \text{ mA}/\text{cm}^2$ at $20.6 \text{ V}/\mu\text{m}$. Then it experiences a sudden drop to $1.43 \text{ mA}/\text{cm}^2$ when the applied field E passes $20.6 \text{ V}/\mu\text{m}$. After that, the current density J steadily increases with the applied field E and does not show saturation or degradation even up to $20 \text{ mA}/\text{cm}^2$ when the field is applied to $50 \text{ V}/\mu\text{m}$. However, when the measurement is repeated at the same location and under the same conditions, the field emission current is turned on at $16 \text{ V}/\mu\text{m}$ and there is no current degradation around $20.6 \text{ V}/\mu\text{m}$. If the measurement is performed at a new location, the current degradation process can be repeated. Apparently, these suffer from a physical breakage in the B_4C nanowires.

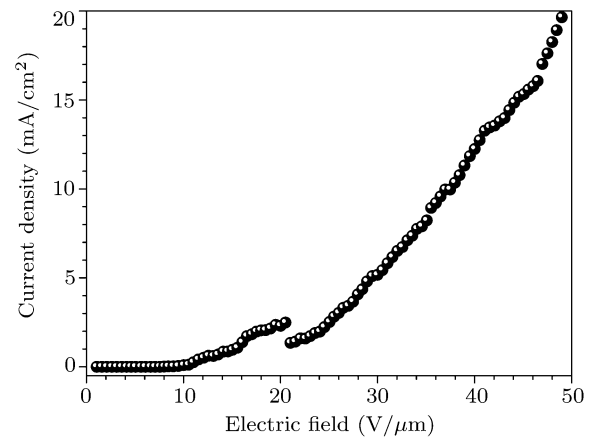


Fig. 5. FE current density J as a function of the applied electric field E for high density boron carbide nanowires. The vacuum gap between the nanowire film and Mo tip is $100 \mu\text{m}$.

We further investigated the field emission properties before and after physical breakage of the nanowire film. The vacuum gap between the film and Mo tip was varied from $300 \mu\text{m}$ to $1000 \mu\text{m}$ at relatively low FE current density (below $1 \text{ mA}/\text{cm}^2$) that was before the current degradation. Figure 6(a) shows the relationships between J and E . It can be concluded that the turn-on field decreases from $3.8 \text{ V}/\mu\text{m}$ to $3 \text{ V}/\mu\text{m}$, corresponding to the vacuum gaps increasing from $300 \mu\text{m}$ to $1000 \mu\text{m}$. This effect is similar to the property of carbon nanotubes in a two-region field-emission model.^[20] Figure 6(b) is the corresponding F-N^[21] plots of the nanowires. It shows that all the plots have nearly the same slopes. From these slopes, the field enhancement factor can be estimated to be 5.0×10^4 . The curves exhibit good linearity, indicating that the FE current originated from barrier-tunnelling electrons extracted by the electric field. The FE stability of the boron carbide nanowires was performed at a distance of $100 \mu\text{m}$ between sample and anode. A field of $15 \text{ V}/\mu\text{m}$ was applied at a chamber pressure of $3.2 \times 10^{-6} \text{ Pa}$ for 2.5 h. Boron carbide nanowires

exhibit a stable long-term emission without obvious fluctuation at relative low FE current density during the test (Fig. 6(c)). The current fluctuation is less than 9% which meets the field emission criterion for display. The field emission property of the nanowires after physical breakage has also been studied. Figure 6(d) shows the $J - E$ curves with different vacuum gaps. The turn-on fields decreases ($16 \text{ V}/\mu\text{m}$ to $6.3 \text{ V}/\mu\text{m}$) with increasing vacuum gaps ($100 \mu\text{m}$ to $1000 \mu\text{m}$), but are larger than those before physical breakage. With a vacuum gap of $100 \mu\text{m}$, the field current reaches $10 \text{ mA}/\text{cm}^2$ when the applied field voltage is increased to 3700 V . The FE characteristics are described by the simplified FN equation.^[21] From these slopes, it can be estimated that the field enhancement factor is 5.0×10^3 . The plots form straight lines, indicating that the FN theory perfectly fits the field emission behaviour of our samples (Fig. 6(e)).

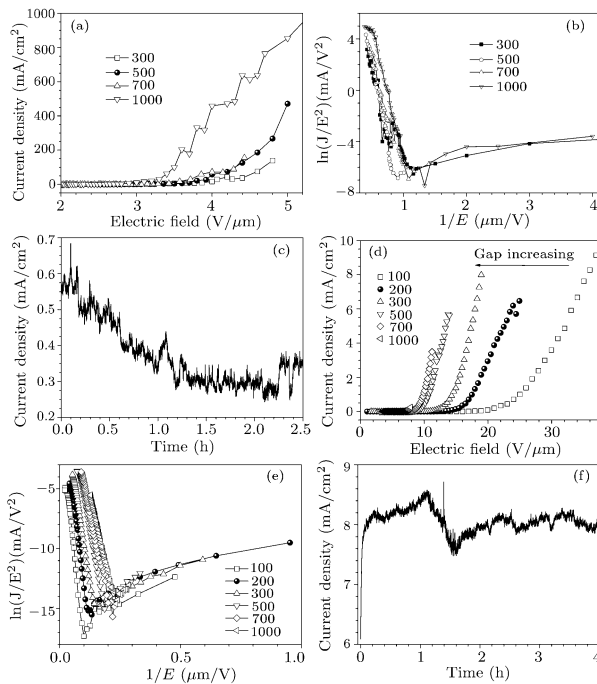


Fig. 6. (a) FE current density J as a function of the applied electric field E from high-density boron carbide nanowires before the physical breakage. (b) FN plots corresponding to (a). (c) FE stability at a sample anode distance of $100 \mu\text{m}$. (d) FE current density J as a function of the applied electric field E after physical breakage. (e) FN plots corresponding to (d). (f) FE stability at a sample-anode distance of $100 \mu\text{m}$.

The FE stability of the B_4C nanowires after physical breakage was tested at a sample anode distance of $100 \mu\text{m}$ and applied field of $40 \text{ V}/\mu\text{m}$ for 4 h with a chamber pressure of $2.0 \times 10^{-6} \text{ Pa}$. Figure 6(f) shows that the high field emission current of B_4C nanowires is very stable with fluctuation below 5% and there is no current decline during a long-term emission. It is more stable than those before their physical breakage (Fig. 6(f)).

The protrusion shown in Fig. 1(c) and the screen-

ing effects may lead to the two-step field emission property. Before physical breakage, these protrusions play an important role in the field emission of the nanowires. Because the protrusions have lower density than the film, the screening effect is weak and it leads to a relative low turn-on field. However, when the applied voltage is increased to a certain value, a high tensile stress exerted by the high local electric field from the high density nanowire emitters. The local Joule heating along the nanowires due to the flow of emission current becomes much higher.^[22] Both the tensile stress^[23] and high temperature^[24,25] lead to break the protrusions and generate a high density flat nanowire array without protrusions. After the physical breakage, due to the high density array of boron carbide nanowires, the screening effect plays an important role in the field emission property, resulting in high turn-on field and lower field enhancement factor than that of an individual nanowire.

In summary, we have developed an improved carbon thermal reduction method to synthesize high density crystalline B_4C nanowires. Field emission characteristic of individual boron carbide nanowire reveal a high field emission current density with an enhancement factor of 10^6 . The evolution process during emission undergoes a thinning of the diameter, enlarging the length of the thin diameter region, and burning the wire breakdown process. Additionally, a high current density two-step field emission property with good stability was found from the nanowires. We believe that all our results together suggest boron carbide nanowires will be useful for flat panel display and semiconductor field emitter applications.

References

- [1] Wood C and Emin D 1984 *Phys. Rev. B* **29** 4582
- [2] Telle R 1994 In *Structure and Properties of Ceramics, Materials Science and Technology* (Weinheim, Germany: VCH) vol 11
- [3] Melmed A J 2007 *Surf. Interface Anal.* **39** 123
- [4] Carlsson M et al 2002 *J. Cryst. Growth* **236** 466
- [5] Han W Q 2006 *Appl. Phys. Lett.* **88** 133118
- [6] Dai H et al 1995 *Nature* **375** 769
- [7] Han W et al 1999 *Chem. Phys. Lett.* **299** 368
- [8] Han W et al 1999 *Chem. Mater.* **11** 3620
- [9] Pender M J and Sneddon L G 2000 *Chem. Mater.* **12** 280
- [10] Zhang D et al 1999 *J. Mater. Sci. Lett.* **18** 349
- [11] Ma R and Bando Y 2002 *Chem. Mater.* **14** 4403
- [12] Yang T Z et al 2005 *J. Phys. Chem. B* **109** 23233
- [13] Wagner R S and Ellis W C 1964 *Appl. Phys. Lett.* **4** 89
- [14] Yu Y et al 2005 *J. Chem. Chem. B* **109** 18772
- [15] Huang Y H et al 2007 *J Phys. Chem. C* **111** 9039
- [16] Zhang H et al 2006 *Adv. Mater.* **18** 87
- [17] Kim J J et al 2007 *Nano Lett.* **7** 2243
- [18] Xu Z et al 2005 *Appl. Phys. Lett.* **87** 163106
- [19] Bonard J M et al 2002 *Phys. Rev. Lett.* **89** 197602
- [20] Zhong D Y et al 2002 *Appl. Phys. Lett.* **80** 506
- [21] Fowler R H et al 1928 *Proc. R. Soc. London A* **119** 173
- [22] Yamamoto S 2006 *Rep. Prog. Phys.* **69** 181
- [23] Bonard J M et al 2001 *Adv. Mater.* **13** 184
- [24] Wei W et al 2006 *Nano Lett.* **7** 64
- [25] Bonard J M et al 2003 *Phys. Rev. B* **67** 115406
Cowburn R P et al 1997 *Appl. Phys. Lett.* **70** 2309